agronomy

Article

Crop Water Requirements and Suitability Assessment in Arid Environments: A New Approach

Abdelrazek Elnashar, Mohamed Abbas, Hassan Sobhy and Mohamed Shahba *

Natural Resources Department, Faculty of African Postgraduate Studies, Cairo University, 12613 Giza, Egypt; abdelrazek.elnashar@cu.edu.eg (A.E.); msaelsarawy@cu.edu.eg (M.A.); hassansobhy20@yahoo.com (H.S.)
* Correspondence: shahbam@cu.edu.eg; Tel.: +20-1093162071

Abstract: Efficient land and water management require the accurate selection of suitable crops that are compatible with soil and crop water requirements (CWR) in a given area. In this study, twenty soil profiles are collected to represent the soils of the study area. Physical and chemical properties of soil, in addition to irrigation water quality, provided data are utilized by the Agriculture Land Evaluation System for Arid and semi-arid regions (ALES-Arid) to determine crop suitability. University of Idaho Ref-ET software is used to calculate CWR from weather data while the Surface Energy Balance Algorithms for Land Model (SEBAL) is utilized to estimate CWR from remote sensing data. The obtained results show that seasonal weather-based CWR of the most suitable field crops (S1 and S2 classes) ranges from 804 to 1625 mm for wheat and berssem, respectively, and ranges from 778 to 993 mm in the vegetable crops potato and watermelon, respectively, under surface irrigation. Mean daily satellite-based CWR are predicted based on SEBAL ranges between 4.79 and 3.62 mm in Toshka and Abu Simbel areas respectively. This study provides a new approach for coupling ALES-Arid, Ref-ET and SEBAL models to facilitate the selection of suitable crops and offers an excellent source for predicting CWR in arid environments. The findings of this research will help in managing the future marginal land reclamation projects in arid and semi-arid areas of the world.

Keywords: crop suitability; remote sensing; ALES-Arid; SEBAL; landsat

Citation: Elnashar, A.; Abbas, M.; Sobhy, H.; Shahba, M. Crop Water Requirements and Suitability Assessment in Arid Environments: A New Approach. *Agronomy* **2021**, *11*, 260. https://doi.org/10.3390/agronomy11020260

Academic Editors: Iván Fco. García-Tejero and Víctor H. Durán-Zuazo

Received: 1 December 2020
Accepted: 28 January 2021
Published: 30 January 2021

1. Introduction

Arid and semi-arid zones represent more than one-third of the land area of the world [1], and are characterized by a long dry season as well as sporadic precipitation [2]. Generally, drylands have been used for livestock production, but recently they are increasingly being used for crop production [3–5]. Egypt lies primarily in arid and semi-arid regions and faces increasing food and water demand. As a result, it struggles to meet its basic food and water needs, due to the continuous increase in population. Increasing crop production without depleting water and land resources in addition to efficient management are significant challenges. The Lake Nasser area in the Aswan governorate of Egypt (22°–24′ N and 31°–33.5′ E) is a good representative for arid and semi-arid environments (Figure 1).

Land suitability is defined as the fitness of a given type of land for specified use, and such suitability can be determined through analytical methods [6–8]. Selecting of a suitable crop is considered an important factor of sustainable agriculture relying on land suitability assessment and also involves assessment of water requirement [9]. Selecting suitable crops for a given area also plays a vital role in efficient water management of time [10,11]. The broad objective of sustainable agriculture is to balance the available land resources with crop requirements, paying particular attention to the optimization of resources used to achieve sustained productivity over a long period [12,13]. Under good management policies in arid regions, the deciding real and exact land resources suitability for specific crop production could likely be more effective and suitable [14].

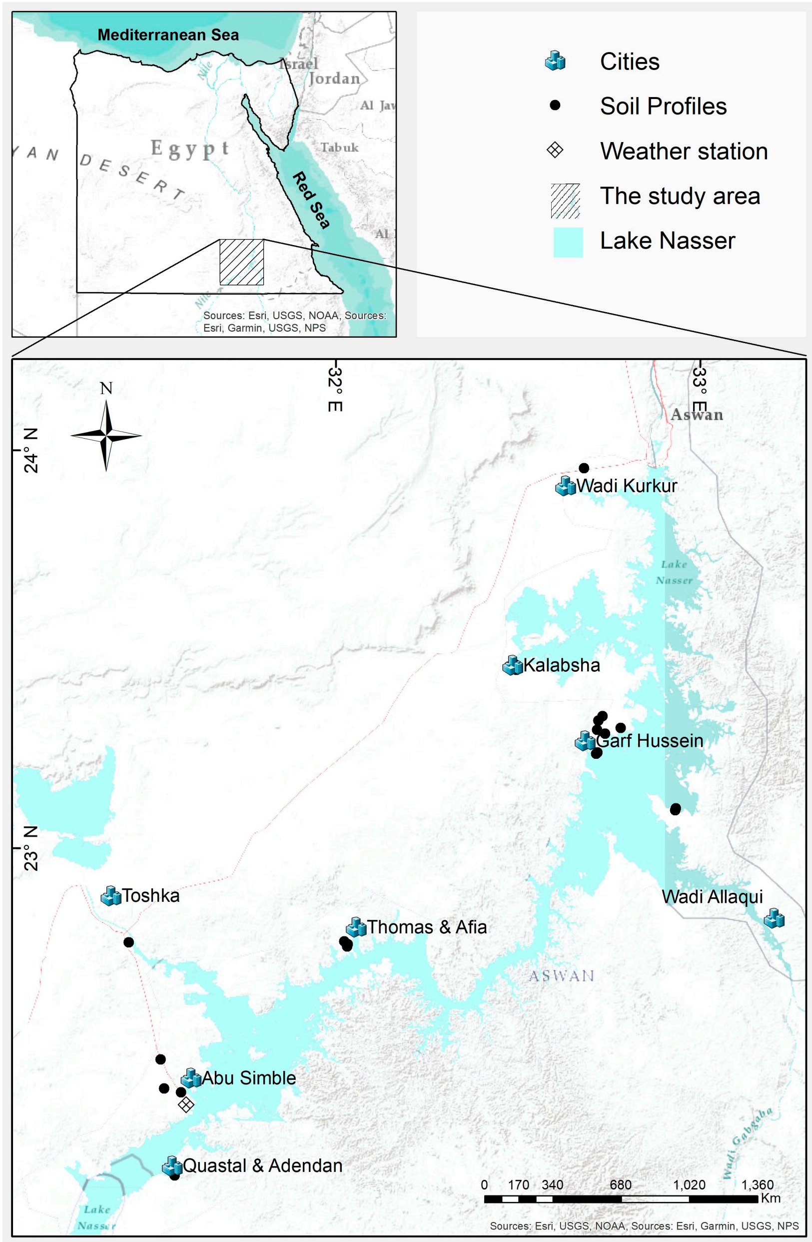

Figure 1. Lake Nasser area, Aswan governorate, Egypt.

Several land evaluation models have been developed to provide a quantified procedure to match land with various actual and proposed uses. For instance, Automated Land Evaluation System (ALES) [6]), Microcomputer-based Mediterranean Land Evaluation Information System (MicroLEIS [15]), Land Evaluation system for Central Ethiopia (LEV-CET [16,17]), Applied System of Land Evaluation and Agricultural Land Evaluation System for arid and semi-arid regions (ASEL/ALES-Arid: [18]), and Agriculture Land Suitability Evaluator (ALSE [19]). However, there is no single or unified land evaluation modelling approach [20,21]. ALESarid-GIS is the updated version of ALES-Arid developed to assess the agricultural land capability and crop suitability in the Geographic Information System (GIS) environment [22]. ALESarid-GIS provides a reasonable solution balancing accuracy, ease of application, and moderate data demand, so its usage has been preferred in evaluating soils for specific crop production in several studies: for instance, in Wahab, et al. [23], Darwish and Abdel Kawy [24], Abd El-Kawy, et al. [25], and Mahmoud, et al. [26]. However, little attention has been paid to estimate the CWR of suitable crops, which is defined by land evaluation for a given area.

Actual evapotranspiration (ETa) is a crucial input to calculate CWR. It can be estimated quite accurately using the aid of weighing lysimeters [27], Eddy correlation [28], and the Bowen ratio [29]. These methods offer potent alternatives for measuring land surface evapotranspiration with high accuracy for a homogeneous area. However, their practical use over large areas is limited due to the number of sites needed to provide point values of evapotranspiration for a specific location. Moreover, it cannot be easily extrapolated to produce accurate maps over a landscape or region. Traditionally, ETa has been estimated by multiplying weather-based reference evapotranspiration (ETr) with crop coefficients (Kc). This method is commonly flawed for multiple reasons. For instance: ETr is a function of weather data alone. Kc values for the same crop showed a significant variation among locations due to differences in crop growth stage, crop variety, soil properties, irrigation method and frequency, climate, and crop management practices. It also does not consider the soil moisture stress level. Furthermore, ETa estimated using this procedure is relatively accurate with an error of $\pm$20% if done well, compared to lysimeters data. Moreover, the accuracy of this methodology is restricted to climatic data, which are not always reliable in many parts of the world [30–32]. However, the role of this method cannot be denied for management and planning purposes—for example, in estimating CWR of the proposed suitable crops for current or newly developed areas.

Therefore, these limitations have encouraged using remotely sensed data to estimate ETa over huge areas. Nowadays, satellite images provide an excellent method for mapping spatial and temporal ETa above the canopy for an entire satellite image. Hence, the estimation of ETa based on remotely sensed data has become a desirable and adequate tool in water resources planning and management [33–36]. Several remote sensing models have been developed to estimate ETa from satellite images particularly at the field/human scale: for instance, the Surface Energy Balance Algorithms for Land Model (SEBAL [37]), Surface Energy Balance System (SEBS [38]), Mapping EvapoTranspiration at High Resolution with Internalized Calibration (METRIC: [30], operational Simplified Surface Energy Balance (SSEBop [39]), and The Atmosphere-Land Exchange Inverse (ALEXI [40]); for more models of remotely sensed ETa see [41–44]. Among these models, SEBAL requires the least amount of inputs with acceptable accuracy. Thus, it has excellent potential for use in developing countries where water management policies are generally inadequate, and ground information is scarce. Moreover, SEBAL has been tested in many countries, especially in arid–semi-arid regions under several different irrigation conditions [45–50].

It is for the abovementioned reasons; this study aims to combine ALESarid, Ref-ET, and SEBAL models as a new and comprehensive approach to improve the selection of suitable crops for available land and water resources, which could be considered the novelty of the current work. This study could be used as a rapid assessment tool to help decision-makers and land managers to prioritize suitable crops based on land and water resources. Section 2 describes the materials and methods. Section 3 presents and discusses the results using data for the area around Lake Naser, Upper Egypt. Conclusions are provided in Section 4.

2. Materials and Methods

2.1. Soil and Water Sampling and Analyses

Twenty representative soil profiles were selected and geo-referenced using the Global Positioning System (GPS) in the study area (Figure 1) around Lake Nasser, Aswan governorate, Egypt (22°–24′ N and 31°–33.5′ E). Soil samples were collected and analyzed in the Laboratories of the Natural Resources Department, Faculty of African Postgraduate Studies, Cairo University in Giza, Egypt, during 2014–2017. Soil physical, chemical, and fertility properties were assessed. Moreover, irrigation water samples representing different soil profiles at 10 cm below the water surface were collected to determine the irrigation water properties. Soil samples were air-dried, ground gently, and sieved through a 2 mm sieve to obtain the fine soil particles. Data of water and soil samples were compiled in ALESarid-GIS system. Physical soil properties (including clay (%), available water (%), hydraulic conductivity (Ks, m/hr), soil depth (cm) and groundwater depth), and chemical soil properties (including soil pH, electrical conductivity (EC, dS/m), cations exchange capacity (CEC, meq/100 g soil), exchangeable sodium percentage (ESP, %), total carbonate (%) and gypsum content (%)) were assessed following USDA [51]. Soil fertility properties (including organic matter (OM, %) and available NPK (ppm)) in addition to irrigation water quality parameters (pH, EC (dS/m), sodium adsorption ratio (SAR), sodium and chloride (meq/L) and boron (B, ppm) were also measured.

2.2. Crop Suitability Using ALESarid-GIS

Soil and water data have been used in the ALESarid-GIS system to assess crop suitability [22]. The evaluation is based on crop suitability affected by the environmental characteristics at the site, such as physical, chemical, and fertility characteristics of the soil, irrigation water quality, and climatic conditions that represent the main factors affecting agricultural soil suitability and productivity in arid and semi-arid regions. Input data of this model are soil physical properties (e.g., soil texture, soil depth, available water and soil permeability), soil chemical properties (e.g., soil salinity, soil alkalinity, calcium carbonate content, gypsum content, cation exchange capacity, and soil reaction), soil fertility properties (e.g., organic matter, available forms of N, P and K), irrigation water characteristics and qualities (e.g., water salinity and toxicity), and finally climate data (e.g., mean summer and winter temperature). Firstly, the model calculates the weighted average value (AV) for each soil property related to a particular soil profile, Equation (1).

$$\mathrm{AV} = \frac{\sum_{i=1}^{n} (v_i \times t_i)}{T} \tag{1}$$

where: v_i is the soil property value relating to soil horizon i; t is the soil horizon thickness (cm), n is the number of horizons within a soil profile, and T is the total soil profile depth (cm). Then, based on the match between the weighted average values of soil parameters and suggested ratings that coded within the model, the land suitability indices and classes for crops were calculated according to the match between the standard crop requirements, which are internally coded data within the model, and various soil parameter levels in the studied area. Finally, the land suitability class was determined by assigning each land suitability index to the confined categories (Table 1). Ismail, Bahnassy and Abd El-Kawy [18] and Abd El-Kawy, Ismail, Rod and Suliman [22] have provided a more detailed description of this model. It is worth noting that ALES-Arid was designed for the arid and semi-arid area. However, for studies in different areas, other land evaluation models can be used (e.g., ALES, MicroLEIS, LEV-CET, and ALSE).

Table 1. Land suitability classes, description and ranges used by ALESarid-GIS.

Class	Description	Rating (%)
S1	Highly suitable	80–100
S2	Moderately suitable	60–80
S3	Marginally suitable	40–60
S4	Conditionally suitable	20–40
NS1	Potentially suitable	10–20
NS2	Actually unsuitable	<10

2.3. Climatic and Remote Sensing Data

Weather data for 2014 were obtained from Abu Simbel weather station located in 22°21′36″ N, 31°36′36″ E with an elevation of 192 m. Data collected were daily minimum and maximum air temperatures, relative humidity, and wind speed. Multi-temporal Landsat-8 images (path 175, row 44) were acquired from earthexplorer.usgs.gov between 20 February and 21 December 2014. Landsat-8 data was provided at the 16-day temporal resolution, 16-bit radiometric resolution, 30 m spatial resolution, LIT processing level (geometric and terrain correction) and free cloud. Satellite image processing was implemented using the geospatial data abstraction library, gdal, [52] in Python programming language.

2.4. Weather-Based CWR Using Ref-ET

Daily reference evapotranspiration (ET_r) was calculated using the University of Idaho Ref-ET software [53,54] as Equation (2).

$$ET_r = \frac{0.408(R_n - G) + \gamma \frac{C_n}{T_a + 273.15} + u_2(e_s - e_a)}{\Delta + \gamma(1 + C_d u_2)} \quad (2)$$

where ET_r is the alfalfa reference evapotranspiration [mm/day]; R_n is the net radiation at the crop surface [MJ/m^2 day]; G is the soil heat flux density at the soil surface [MJ/m^2 day]; T_a is the mean daily or hourly air temperature at 1.5–2.5 m height [C]; u_2 is the mean daily wind speed at 2 m height [m/s]; e_s is the saturation vapor pressure at 1.5–2.5 m height [KPa]; e_a is the actual vapour pressure at 1.5–2.5 m height [KPa]; Δ is the slope of the saturation vapor pressure-temperature curve [KPa/C]; γ is the psychometric constant [KPa/C]; C_n is the numerator constant that changes with reference type and calculation time step; C_d is the denominator constant that changes with reference type and calculation time step; 0.408 coefficient [m^2 mm/MJ]. Cumulative ETa and CWR [55] were estimated by Equations (3) and (4) respectively.

$$\mathrm{ET_{a\ Cumulative-WB}} = \sum_{i=1}^{n} \mathrm{ET_r\ K_{cr}} \quad (3)$$

$$\mathrm{CWR}_{WB} = \mathrm{ET_{a\ Cumulative-WB}} \ / \ \text{Irrigation efficiency} \quad (4)$$

where $\mathrm{ET_{a\ Cumulative}}$ is the weather-based cumulative $\mathrm{ET_a}$ [mm] from the day i through the day n; $\mathrm{ET_r}$ is the reference ET [mm] for the day i from Equation (2); $\mathrm{K_{cr}}$ is the alfalfa-based single crop coefficient [dimensionlessfor the day i, irrigation efficiency ranging between 0 and 1, and CWR_{WB} is the weather-based crop water requirement [mm].

2.5. Satellite-Based CWR Using SEBAL

Extensive SEBAL formulation is available in its original literature [37,56–58], so here we introduce a short description of the SEBAL model. Landsat-8 data converted from digital numbers to reflectance and radiance to calculate vegetation indices, surface albedo, and surface temperatures following [59]. It is worth noting that the SEBAL Calibrated using Inverse Modeling of Extreme Conditions (CIMIC) approach is used to generate image-date specific sensible heat flux (H) map where CIMIC effectively minimizes systematic biases in Rn, G, Ts, and $\mathrm{Z_{0m}}$ [37]. $\mathrm{ET_a}$ is predicted from the residual amount of energy remaining from the energy balance that includes all major sources ($\mathrm{R_n}$) and consumers (G, H and LE) of energy as Equation (5):

$$\mathrm{R_n} - \mathrm{G} - \mathrm{H} - \mathrm{LE} = 0 \quad (5)$$

where $\mathrm{R_n}$ is the net radiation, H is the sensible heat, G is the soil heat flux, LE is the latent heat flux. All are instantaneous values in [W/m^2]. Net radiation was calculated as Equation (6):

$$\mathrm{R_n} = (1 - \alpha)\mathrm{R_{S\downarrow}} + \mathrm{R_{L\downarrow}} - \mathrm{R_{L\uparrow}} - (1 - \varepsilon_0)\mathrm{R_{L\downarrow}} \quad (6)$$

where α is the surface albedo [dimensionless]; $\mathrm{R_{S\downarrow}}$ is the incoming short-wave radiation [W/m^2]; $\mathrm{R_{L\downarrow}}$ is the incoming longwave radiation [W/m^2]; $\mathrm{R_{L\uparrow}}$ is the outgoing longwave radiation [W/m^2]; ε_0 is the broad-band surface emissivity [dimensionless]. Soil heat flux calculated as Equation (7):

$$\mathrm{G} = \left(((\mathrm{Ts} - 273.15)/\alpha)\left(0.0038\alpha + 0.0074\alpha^2\right)\left(1 - 0.98\mathrm{NDVI}^4\right)\right)\mathrm{R_n} \quad (7)$$

where Ts is the surface temperature [K]; NDVI is the Normalized Differences Vegetation Index [dimensionless].

Momentum roughness length was calculated as Equation (8):

$$Z_{0m} = \exp[(a\ \mathrm{NDVI}/\alpha) + b] \tag{8}$$

where Z_{0m} is the momentum roughness length [m]; a and b are regression constants derived from a plot of initial $\ln(Z_{0m})$ vs NDVI/α [56]. These two parameters should be defined by the SEBAL operator, thus, they play an important role in the model performance. Sensible heat flux calculated as Equation (9):

$$H = \rho_a\ C_P(dT/r_{ah}) \tag{9}$$

where ρ_a is the air density [Kg/m^3]; C_P is the specific heat [J/Kg $\times$ K]; r_{ah} is the aerodynamic resistance for heat transport [s/m]. The relationship between the temperature differences and remotely sensed surface temperature is very close as Equation (10):

$$dT = a\ T_s + b \tag{10}$$

where dT is the temperature differences between two heights at 0.1 m and 2 m above the canopy [K]; a $[-]$, b$[K]$ are the calibration coefficients derived using the cold and hot pixels site and time-specific candidates. It should be highlighted that cold and hot pixels location are operator-specific, which means a SEBAL operator has to define these two locations for each image carefully as described, in detail, in SEBAL literature.

Once the instantaneous net radiation, soil heat flux, and sensible heat flux were determined, the instantaneous latent heat flux was estimated at the moment of satellite overpass on a pixel-by-pixel level, then converted to an equivalent amount of water depth. The instantaneous evaporative fraction was calculated as Equation (11):

$$\Lambda = LE/R_n - G \tag{11}$$

Evaporative fraction expresses the ratio of actual to crop evaporative demand when atmospheric moisture conditions are in equilibrium with soil moisture conditions [60]. Studies have shown that the evaporative fraction remains constant throughout the day [61,62]. Therefore, daily ET_a was calculated from the energy balance equation as Equation (12):

$$ET_{a24} = 86400\ \Lambda\ (R_{n24} - G_{24})/\lambda \tag{12}$$

where: Λ is the evaporative fraction [dimensionless]; R_{n24} is the daily net radiation calculated on a daily time step [W/m^2]; G_{24} is the daily soil heat flux [W/m^2]; λ is the latent heat of vaporization [J/kg]; 86400 is a time conversion from seconds to days. The daily ET_a for the entire image area changes in proportion to the change in the daily ET_r on the index weather site [30,63]. Thereby, Cumulative ET_a calculated as Equation (13):

$$ET_{a\ \mathrm{Cumulative-RS}} = \sum_{i=1}^{n} (ET_{a24})_i \times (K_m)_i \tag{13}$$

$$K_m = (ET_{r\ \mathrm{cumulative}}/ETr_i) \tag{14}$$

where $ET_{a\ \mathrm{Cumulative-RS}}$ is the remotely sensed cumulative ET_a [mm] from the day i through the day n; ET_{a24} is the daily ET_a [mm] for day i; $ETrF_{24}$ is the daily ET_r fraction [mm] for day i; K_m is multiplier [dimensionless] for each period to convert ET_a for the day of the image into ET_a for the period; $ET_{r\ \mathrm{Cumulative}}$ is the cumulative reference ET [mm] for the period; ETr_i is the reference ET [mm] for day i. Finally, remote sensing CWR can be estimated as Equation (15):

$$CWR_{RS} = ET_{a\ \mathrm{Cumulative-RS}} \tag{15}$$

where $ET_{a\ Cumulative-RS}$ is the remotely sensed cumulative ET_a [mm] from the day i through the day n; and CWR_{RS} is the remote sensing CWR [mm].

3. Results and Discussion

3.1. Soil and Irrigation Water Properties

Soil analysis indicated low clay content, low water availability, and high hydraulic conductivity (Table 2). Most of the investigated soil could be considered as alkaline and non-saline with low CEC. These results are in agreement with those obtained by previous studies [64–66]. In accordance with Khalifa [64], and Abbas, El-Husseiny, Mohamed and Abuzaid [65], soil OM content was very low, and the available NPK values were not sufficient. The difference in soil properties may be due to the variability of topography and parent rocks. Taghizadeh-Mehrjardi, et al. [67] assessed land suitability in Kurdistan province in Iran for crop production and conclude that the differences in soil characteristics were due to variability in topography, climate, and parent material. Additionally, they considered topography and climate data as the essential auxiliary data for predicting land suitability class.

Table 2. Soil depth (SD), clay content average (%), available water (AW, %), hydraulic conductivity (Ks, m/hr), total carbonates (TC, %), gypsum content (GC, %), exchangeable sodium percentage (ESP, %), soil pH, cations exchangeable capacity (CEC, meq/100 g soil) electrical conductivity (EC, dS/m), organic matter (OM, %) and available nitrogen (N, ppm), phosphorous (P, ppm) and potassium (K, ppm).

ID	SD	Clay	AW	Ks	TC	GC	ESP	pH	CEC	EC	OM	N	P	K
1	85	0.72	2.48	0.63	2.21	0.08	13.96	7.82	3.32	2.09	0.04	0.11	0.28	2.12
2	90	8.10	2.80	0.22	1.70	0.07	12.20	8.11	6.30	1.20	0.03	0.13	0.23	1.90
3	90	8.12	2.64	0.22	1.86	0.06	11.63	8.12	6.41	1.25	0.04	0.11	0.33	1.88
4	95	7.93	2.80	0.23	1.83	0.05	14.43	8.05	6.17	1.27	0.04	0.10	0.40	2.80
5	95	5.55	2.61	0.37	1.05	0.06	5.34	7.74	5.64	0.90	0.05	0.14	0.52	2.89
6	90	1.00	2.63	0.62	2.50	0.07	14.07	7.76	3.80	2.32	0.03	0.07	0.23	1.47
7	70	7.93	3.03	0.23	1.63	0.05	11.81	7.63	6.39	2.45	0.01	0.04	0.13	0.77
8	90	5.95	2.50	0.34	1.10	0.08	5.25	7.67	5.15	0.79	0.04	0.05	0.30	2.05
9	95	5.64	2.11	0.36	0.99	0.07	4.88	7.72	5.06	0.94	0.04	0.04	0.31	1.60
10	90	5.05	1.90	0.39	1.05	0.07	4.80	7.60	4.95	0.89	0.05	0.06	0.25	1.90
11	90	1.50	2.70	0.59	3.80	0.07	20.10	7.95	3.05	2.87	0.05	0.15	0.65	3.05
12	85	6.94	2.94	0.29	1.75	0.06	14.06	8.08	5.44	0.64	0.04	0.12	0.48	2.35
13	90	5.60	2.00	0.36	1.10	0.06	4.80	7.61	4.55	3.45	0.05	0.15	0.55	2.60
14	95	1.64	2.54	0.58	3.81	0.07	4.99	7.86	2.99	2.81	0.06	0.15	0.66	2.21
15	80	0.78	1.51	0.63	2.29	0.07	12.28	7.88	2.60	1.27	0.03	0.04	0.19	2.18
16	50	1.72	2.54	0.58	3.44	0.06	11.14	8.66	2.82	1.97	0.04	0.14	0.36	3.04
17	85	6.44	3.32	0.32	1.71	0.06	12.82	8.08	5.51	0.62	0.04	0.10	0.37	1.56
18	90	6.80	3.24	0.30	1.71	0.07	13.83	7.68	5.59	3.06	0.06	0.18	0.62	4.00
19	95	6.94	3.37	0.29	1.58	0.07	13.76	7.59	5.85	3.47	0.04	0.05	0.14	1.37
20	60	11.00	2.95	0.06	4.60	0.07	12.05	7.89	7.00	4.72	0.06	0.10	0.55	2.45
Min	50.00	0.72	1.51	0.06	0.99	0.05	4.80	7.59	2.60	0.62	0.01	0.04	0.13	0.77
Max	95.00	11.00	3.37	0.63	4.60	0.08	20.10	8.66	7.00	4.72	0.06	0.18	0.66	4.00
Mean	85.50	5.27	2.63	0.38	2.09	0.07	10.91	7.88	4.93	1.95	0.04	0.10	0.38	2.21
SD	11.82	2.94	0.47	0.16	1.02	0.01	4.25	0.25	1.34	1.13	0.01	0.04	0.16	0.71
CV (%)	13.83	55.73	17.68	42.95	48.79	12.12	38.98	3.21	27.09	57.95	27.77	42.29	43.49	32.16

Irrigation water properties for all collected samples were similar among different sectors (Table 3). This result was expected as irrigation water came from the same source (Lake Nasser), which has high-quality irrigation water for the proposed crops according to FAO [68] and El-Mahdy, et al. [69], who indicated the suitability of Lake Naser water for drinking and irrigation. These findings also are found to be in agreement with previous work of Fayed, et al. [70]. They tested the chemical properties of Lake Nasser water and found that the concentration of elements in Lake Nasser water was within the permissible limits.

Table 3. Irrigation water properties in the study area.

Samples	EC (dS/m)	pH	SAR	Na^+ (meq/L)	Cl^{-1} (meq/L)	B^{-1} (ppm)
1	0.20	8.38	3.92	3.30	1.20	0.02
2	0.20	8.53	4.28	3.37	1.00	0.13
3	0.24	7.79	3.31	3.13	1.20	0.08
4	0.24	7.32	3.54	3.19	1.20	0.04
5	0.21	7.37	3.67	3.13	1.00	0.11
6	0.19	7.67	3.16	2.85	1.20	0.11
7	0.22	7.67	3.16	2.92	2.20	0.07
8	0.71	6.85	2.99	4.31	1.80	0.03
Min	0.19	6.85	2.99	2.85	1.00	0.02
Max	0.71	8.53	4.28	4.31	2.20	0.13
Mean	0.27	7.70	3.50	3.27	1.35	0.08
SD	0.16	0.52	0.41	0.43	0.40	0.04
CV (%)	59.48	6.71	11.70	13.00	29.40	53.04

3.2. Crop Suitability Assessment Using ALESarid-GIS

Crop suitability is divided into five classes: S1, S2, S3, S4, and NS2, indicating highly suitable, moderately suitable, marginally suitable, conditionally suitable and unsuitable, respectively. Table 4 previews land suitability for 28 field crops in the study area. Since the total number of soil profiles are 20 profiles and each soil profile covers a different area, crop suitability class (%) is calculated as n of soil profiles in each class divided by the total number of soil profiles. For instance, wheat crop classified as S1 (highly suitable) for four soil profiles (2, 3, 4, and 20), thus, wheat is highly suitable for 20% of the study area. Based on S1 and S2 classes of suitability, alfalfa and sorghum were the highest suitable crops (95%), followed by onion, wheat and barley (90%), sugar beet (80%), sugarcane, peppers, and watermelons (70%), and pear (50%). Some crops were found to be completely unsuitable such as date palm, fig, olives, grapes, citrus, tomatoes, cabbage, peas, peanuts, and rice (Table 4). According to Aswan governorate statistical guide [71], most of these crops are actually planted in the study area indicating the validity of ALESarid estimates. At the same time, there are other crops not included in ALESarid database but cultivated in the study area (i.e., eggplant, courgettes, garlic, okra, spinach, corchorus, hibiscus, henna, sesame and fenugreek). Similar findings were reported by Hassan, et al. [72], who studies land suitability for wheat, maize, potatoes, sugar beet, alfalfa, peach, citrus, and olive in Hala'ib and Shalateen regions, South-Eastern of the study area.

3.3. Weather-Based CWR

Monthly reference evapotranspiration (ET_r) increased from January to July, then gradually decreased to reach its minimum in December (Figure 2). Monthly ET_r was 5.79, 10.94, and 4.80 mm/day in January, July, and December, respectively. There was a positive association between the change in ET_r and the change in air temperature. The difference in ET_r was negatively associated with the change in humidity. Data collected from the nearest weather station agreed with our findings. Crop water requirements (CWR) were calculated based on 60%, 75%, and 85% efficiency for surface, sprinkler and drip irrigation respectively [73]. Crop coefficient (Kc) values, planting date and harvesting date were obtained from the previous studies [74–77].

Table 4. Land suitability for 28 field crops around Lake Nasser, Aswan, Egypt, determined during 2014–2017.

Crop	**Soil Profiles**																				**Classes %**				
																					S1	**S2**	**S3**	**S4**	**NS2**
	1	**2**	**3**	**4**	**5**	**6**	**7**	**8**	**9**	**10**	**11**	**12**	**13**	**14**	**15**	**16**	**17**	**18**	**19**	**20**					
Wheat/Barley	S3	S1	S1	S1	S2	S2	S2	S2	S2	S2	S2	S2	S2	S2	S3	S2	S2	S2	S2	S1	20	70	10	0	0
Faba bean	S3	S3	S3	S3	S2	S3	S3	S2	S2	S2	S3	S2	S2	S2	S3	S2	S2	S2	S2	S3	0	55	45	0	0
Sugarbeet	S3	S2	S2	S2	S2	S3	S2	S2	S2	S2	S3	S2	S2	S2	S3	S2	S2	S2	S2	S1	5	75	20	0	0
Sunflower	S3	S3	S3	S3	S2	S3	S3	S2	S2	S2	S3	S3	S2	S3	S3	S3	S3	S2	S2	S3	0	35	65	0	0
Rice	NS2	NS2	NS2	NS2	NS2	NS2	NS2	NS2	NS2	NS2	NS2	NS2	NS2	NS2	NS2	NS2	NS2	NS2	NS2	NS2	0	0	0	0	100
Maize/Soybean	S3	S3	S3	S3	S2	S3	S3	S2	S2	S2	S3	S2	S2	S2	S3	S3	S2	S2	S2	S3	0	50	50	0	0
Peanut/Cabbage/Peas/Tomato	S3	S3	S3	S3	S3	S3	S3	S3	S3	S3	S3	S3	S3	S3	S3	S3	S3	S3	S3	S3	0	0	100	0	0
Cotton	S3	S3	S3	S3	S2	S2	S3	S2	S2	S2	S2	S2	S2	S2	S3	S3	S2	S2	S2	S3	0	60	40	0	0
Sugarcane	S3	S2	S2	S2	S2	S3	S2	S2	S2	S2	S3	S2	S2	S3	S3	S4	S2	S2	S2	S2	0	70	25	5	0
Onion	S3	S1	S1	S1	S2	S2	S2	S2	S2	S2	S2	S2	S2	S2	S3	S2	S2	S2	S2	S2	15	75	10	0	0
Potato	S3	S3	S3	S3	S3	S3	S3	S3	S2	S3	S3	S3	S3	S3	S3	S3	S3	S3	S3	S3	0	5	95	0	0
Peppers/Watermelon	S3	S3	S3	S3	S2	S2	S3	S2	S2	S2	S2	S2	S2	S2	S2	S2	S2	S2	S2	S3	0	70	30	0	0
Alfalfa/Sorghum	S3	S1	S1	S1	S1	S2	S1	S1	S1	S2	S2	S1	S2	S2	S2	S2	S2	S2	S1	S1	50	45	5	0	0
Citrus/Grape/Fig	NS2	S3	S3	S3	S3	S4	NS2	S3	S3	S3	S4	NS2	S3	S3	NS2	NS2	NS2	S3	S3	NS2	0	0	55	10	35
Banana	NS2	S3	S3	S3	S2	S3	NS2	S2	S2	S2	S3	NS2	S3	S3	NS2	NS2	NS2	S3	S3	NS2	0	20	45	0	35
Olives	NS2	S3	S3	S3	S3	S3	NS2	S3	S3	S3	S3	NS2	S3	S3	NS2	NS2	NS2	S3	S3	NS2	0	0	65	0	35
Apple	NS2	S3	S3	S3	S2	S3	NS2	S2	S2	S2	S3	NS2	S3	S3	NS2	NS2	NS2	S3	S2	NS2	0	25	40	0	35
Pear	NS2	S2	S2	S2	S2	S3	NS2	S2	S2	S2	S3	NS2	S2	S3	NS2	NS2	NS2	S2	S2	NS2	0	50	15	0	35
Date Palm	NS2	S3	S3	S3	S3	S3	NS2	S3	S3	S3	S3	NS2	S3	S3	NS2	NS2	NS2	S3	S3	NS2	0	0	65	0	35

S1 (green), S2 (blue), S3 (orange), S4 (yellow) and NS2 (red) indicate highly suitable, moderately suitable, marginally suitable, conditionally suitable, and unsuitable, respectively.

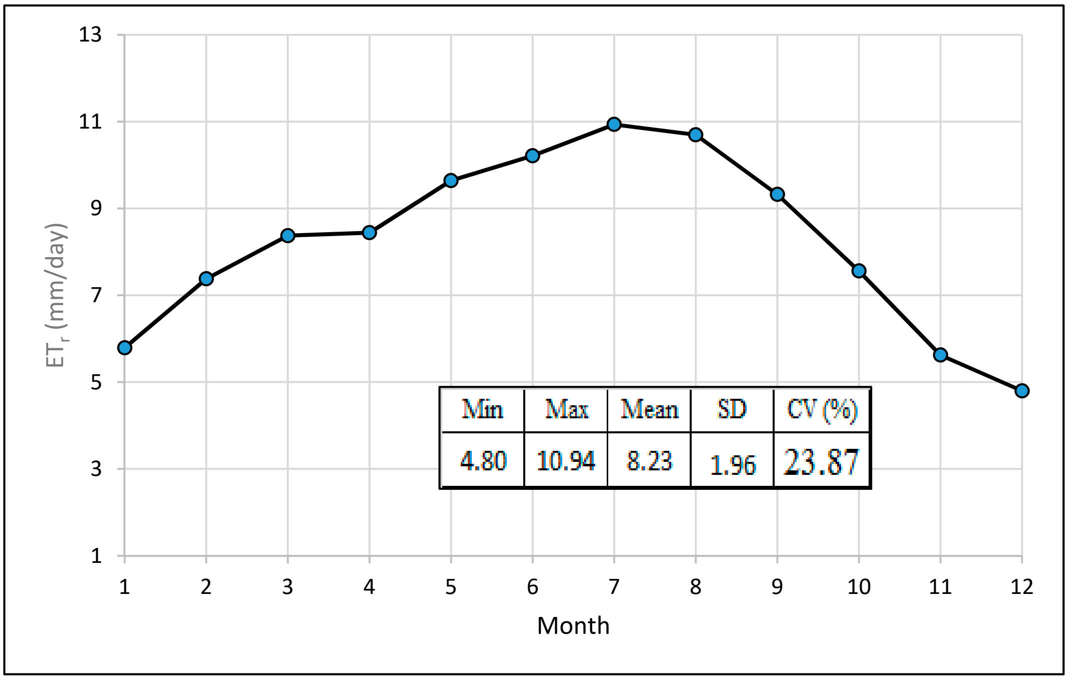

Figure 2. Monthly reference evapotranspiration (ET_r; mm/day) based on daily time step climatic data from Abu Simbel weather station (22°21′36″ N, 31°36′36″ E) for 2014.

Land suitability level for 28 field crops around Lake Nasser in Aswan, Egypt, determined during 2014–2017 was graphically presented in Table 4. Crop water requirements for summer field crops ranged from 820 to 3406 mm for sunflower and sugarcane, while it ranged for winter crops from 658 to 1625 mm for faba bean and berssem (5 cuts), respectively (Table 5).

Table 5. Crop water requirements for field crops, vegetable crops, and fruit trees under different irrigation systems.

					Surface	**Sprinkler**	**Drip**
Crop	**Days**	**Planting Date**	**Harvesting Date**	**ETa (mm)**		**CWR (mm)**	
			Summer field crops				
Sunflower	90	01/05/2014	30/07/2014	492	820	656	579
Sorghum	120	15/05/2014	12/09/2014	675	1126	900	
Maize	120	15/04/2014	13/08/2014	680	1133	906	799
Peanut	120	15/04/2014	13/08/2014	697	1162	930	820
Sugarcane	365	01/02/2014	01/02/2015	2044	3406	2725	2405
Soybean	123	01/05/2014	01/09/2014	641	1069	855	755
			Winter field crops				
Wheat	165	01/11/2014	15/04/2015	482	804	643	
Barley	150	15/10/2014	14/03/2015	482	803	643	
Berssem	240	15/09/2014	13/05/2015	975	1625	1300	
Faba bean	122	01/11/2014	03/03/2015	395	658	527	465
Onion	151	01/10/2014	01/03/2015	485	808	646	570
			Annual field crops				
Alfalfa	365	01/01/2014	01/01/2015	2025	3374	2699	2382

Table 5. *Cont.*

Crop	Days	Planting Date	Harvesting Date	ETa (mm)	Surface	Sprinkler	Drip
						CWR (mm)	
Summer vegetable crops							
Watermelon	122	01/03/2014	01/07/2014	596	993	794	701
Peppers	153	01/04/2014	01/09/2014	793	1321	1057	933
Cabbage	153	15/04/2014	15/09/2014	783	1305	1044	921
Tomato	150	15/01/2014	14/06/2014	678	1130	904	797
Potato	120	01/02/2014	01/06/2014	544	907	726	640
Winter vegetable crops							
Cabbage	151	15/10/2014	15/03/2015	483	806	644	569
Tomato	151	15/09/2014	13/02/2015	529	882	705	622
Potato	123	01/10/2014	01/02/2015	389	648	518	457
Peppers	150	01/10/2014	28/02/2015	481	801	641	566
Peas	150	15/09/2014	12/02/2015	490	816	653	576
Deciduous fruit trees							
Grape	275	01/3/2014	01/12/2014	933	1555	1244	1098
Fig	275	01/3/2014	01/12/2014	948	1579	1263	1115
Evergreen fruit trees							
Date Palm	365	01/01/2014	01/01/2015	1119	1865	1492	1316
Olives	365	01/01/2014	01/01/2015	1119	1865	1492	1316
Citrus	365	01/01/2014	01/01/2015	1548	2581	2065	1822
Banana	365	01/01/2014	01/01/2015	2022	3369	2695	2378

Summer and winter vegetable crop harvests varied significantly for the same crop. For a summer harvest, CWR ranged from 907 to 1321 mm, and for winter harvest ranged from 648 to 882 mm in potato and tomato, respectively (Table 5). Crop water requirements for deciduous fruit trees varied from 1555 to 1579 mm for grape and fig, respectively, and ranged from 1865 to 3369 mm in the evergreen fruit trees date palm and banana, respectively. These findings can be confirmed by the study of Mahmoud and El-Bably [78]. Precise predictions of CWR depend on accurate crop ET assessment, accessible satellite images source and precise forecasting of meteorological data [79].

3.4. Weather-Based CWR of Suitable Crops

Crop suitability that represented by S1 and S2 classes along with their CWR (Table 6) indicated that the range of CWR for the most suitable field crops is between 804 and 1625 mm for wheat and berssem (5 cuts), respectively. Vegetable crops CWR ranged from 778 to 993 mm for potato and watermelon, respectively. For banana trees, CWR was 3369 mm under surface irrigation. ALESarid-GIS output based on soil and water properties indicated that sugar beet, cotton, apple, and pear are the most suitable crops. However, based on the physiological demand of these crops, they cannot grow in the study area because of other factors, such as climatic conditions. At the same time, date palm that was proven as unsuitable (S3) is successfully cultivated in the study area. In arid regions, a suitable cropping pattern for an area could be decided based on both the actual and potential status of the area defined by land suitability indices for different crops [14] while Abd El-Hady and Abdelaty [80] indicated that crops soil suitability is mainly determined by soil properties, crop rooting depth, and crops salinity tolerance. However, this study highly recommends integrating CWR of the most suitable crops for a region to ensure a real match between these crops and water availability for irrigation.

Table 6. Crop water requirements (CWR) of the most suitable crops under the surface, sprinkler, and drip irrigation systems.

			Surface	**Sprinkler**	**Drip**
Crop	**S1%**	**S2%**		**CWR [mm]**	
			Field crops		
Faba bean		55	658	527	465
Wheat	20	70	804	643	
Barley	20	70	803	643	
Sunflower		35	820	656	579
Maize		50	1133	906	799
Sugarbeet	5	75			
Soybean		50	1069	855	755
Onion	15	75	808	646	570
Berssem	50	45	1625	1300	
Alfalfa	50	45	3374	2699	
Cotton		60	-		
			Vegetable crops		
Potato		5	778	622	549
Watermelon		70	993	794	701
			Fruit trees		
Apple		25			
Pear		50			
Banana		20	3369	2695	2378

3.5. Actual CWR Using SEBAL

Calculations of ET_a based on remotely sensed data and SEBAL approach were done with sprinkler and surface irrigation systems in Toshka and Abu Simbel locations, respectively (Figure 3). Those two locations were selected to investigate the applicability of remote sensing data with the SEBAL model in CWR estimation, given that they represent two different irrigation and management systems and cover most of the study area. The essential elements in SEBAL are the sensible heat flux and the momentum roughness length calculation, which depend upon the operator, time, and site-specific parameters; coefficients a and b in Equations (8) and (10). These coefficients are defined for each day-image and presented in Table A1. Paula, et al. [81] assured that the atmospheric stability conditions ensure reasonable estimates of ETa.

From Figure 3, ETa spatial variations between Toshka and Abu Simbel locations can be attributed to the differences in the land and water management in each location where more water is consumed at Toshka location because of the well-managed agriculture system (e.g., sprinkler irrigation) compared with that at Abu Simbel location (flood irrigation). Figure 4 presents daily ET_a at cold pixels, mean daily ETa at Toshka and Abu Simbel locations, as well as weather-based ET_r calculated based on weather data from the Abu Simbel weather station. Daily ET_a at cold pixels represents a well-watered vegetation condition that has a minimum surface temperature (Ts) above the canopy with maximum vegetation cover (NDVI) and surface albedo (α). In this situation, the temperature difference (dT) is minimal or zero and this leads to sensible heat flux (H) that has become minimal or zero too. Latent heat flux (LE) and the evaporative fraction (Λ) becomes a maximal rate due to all the available energy consumed in the latent heat flux [30,37]. Thus, these cold pixel values refer to well-managed fields. Compared to the temporal change in daily ET_a at cold pixels versus mean daily ETa at Toshka and Abu Simbel locations: (1) The mean daily ETa at Abu Simbel location is always lower than at Toshka location, and (2) the mean daily ETa at Toshka location is very close to daily ET_a at cold pixels confirming the results that obtained in Figure 3 and Table 7. Remotely sensed CWR of each cultivated crop could be achieved by using a crop type map. Unfortunately, this map is not available for this study to precisely compare between weather-based and remote sensing-based CWR, which is highly recommended in future studies. However, daily ETr from Figure 4 and Table 7 is higher than ETa by about 50% with SD and CV reaching 2.4 and 26.92% respectively, thus indicating, in general, a higher estimation of weather-based CWR (Table 4; Table 5). Therefore, the calculation of ETa using satellite data and SEBAL model is useful for guiding the daily operation of water management in the arid region [82]. Moreover, Sun, et al. [83] demonstrated the considerable potential of the SEBAL model for estimation of spatial ETa with little ground-based weather data over large areas at the field scale. These findings also can be confirmed by the mean NDVI spatial variation maps (Figure 5). The maximum NDVI values were clustered over Toshka at 0.80 (mean = 0.33; CV = 40%) while at Abu Simbel it was at 0.73 (mean = 0.27; CV = 42%). Both ETa and NDVI spatial variation maps are completely agreed with each other where lower ETa (NDVI) with higher CV value mapped over Abo Simbel and higher ETa (NDVI) with lower CV value clustered over Toshka.

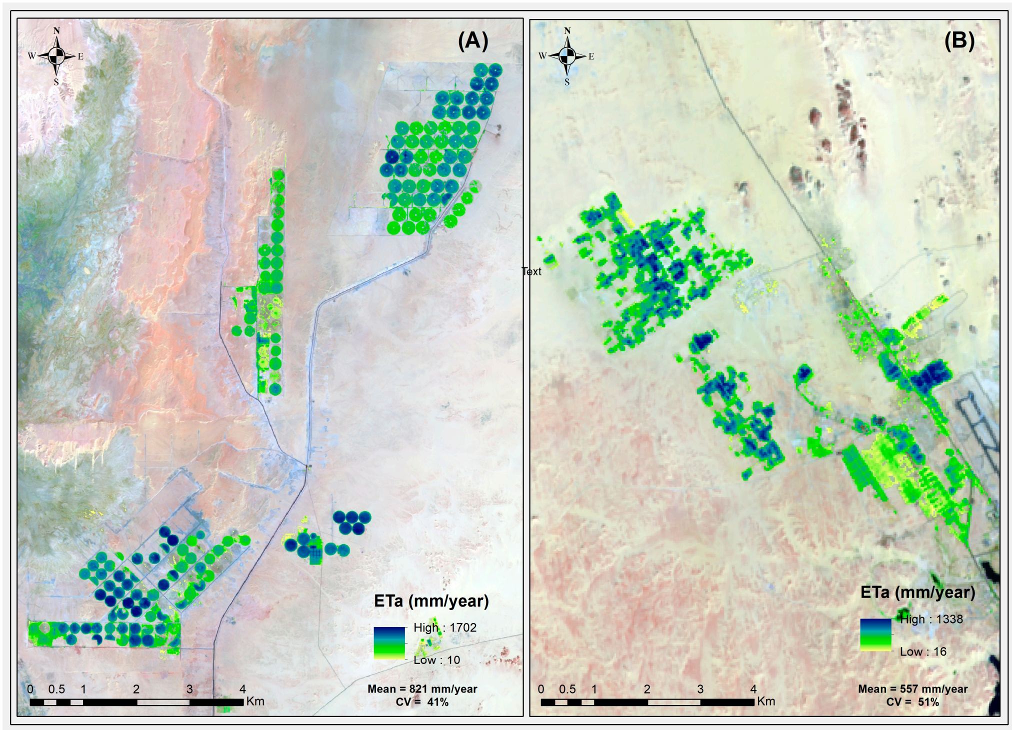

Figure 3. Annual actual evapotranspiration (mm) at Toshka (**A**) and Abu Simbel (**B**) for 2014.

Table 7. Minimum, maximum, mean, standard deviation (SD) and coefficient of variation (CV) of daily ETa at cold pixels, mean daily ETa at Toshka and Abu Simbel locations and weather-based ET_r.

	ETa (mm)			ETr
	Cold Pixels	**Toshka**	**Abu Simbel**	
Minimum	2.81	2.40	2.74	4.49
Maximum	5.74	6.56	4.77	13.40
Mean	4.73	4.79	3.62	8.90
SD	0.88	1.08	0.69	2.40
CV (%)	18.53	22.67	19.16	26.92

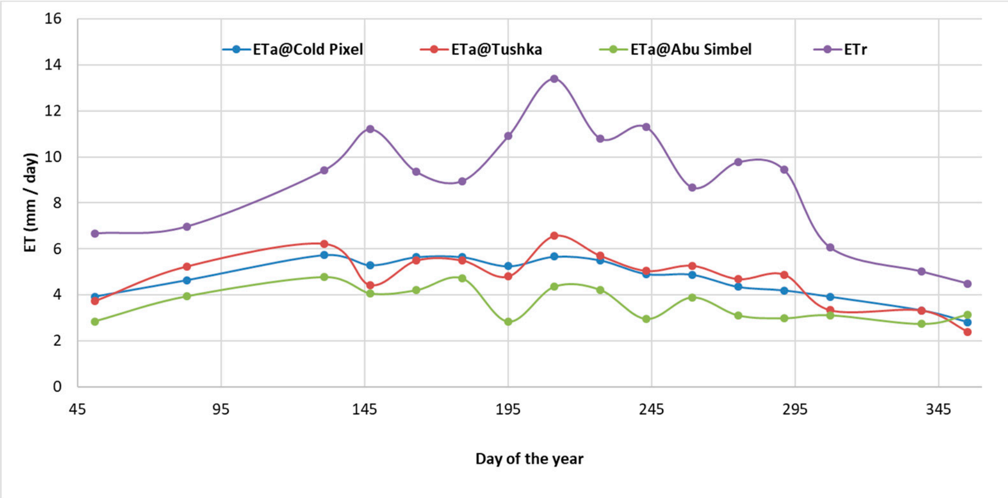

Figure 4. Daily ET_a at cold pixels, mean daily ETa at Toshka and Abu Simbel locations and weather-based ET_r for 2014.

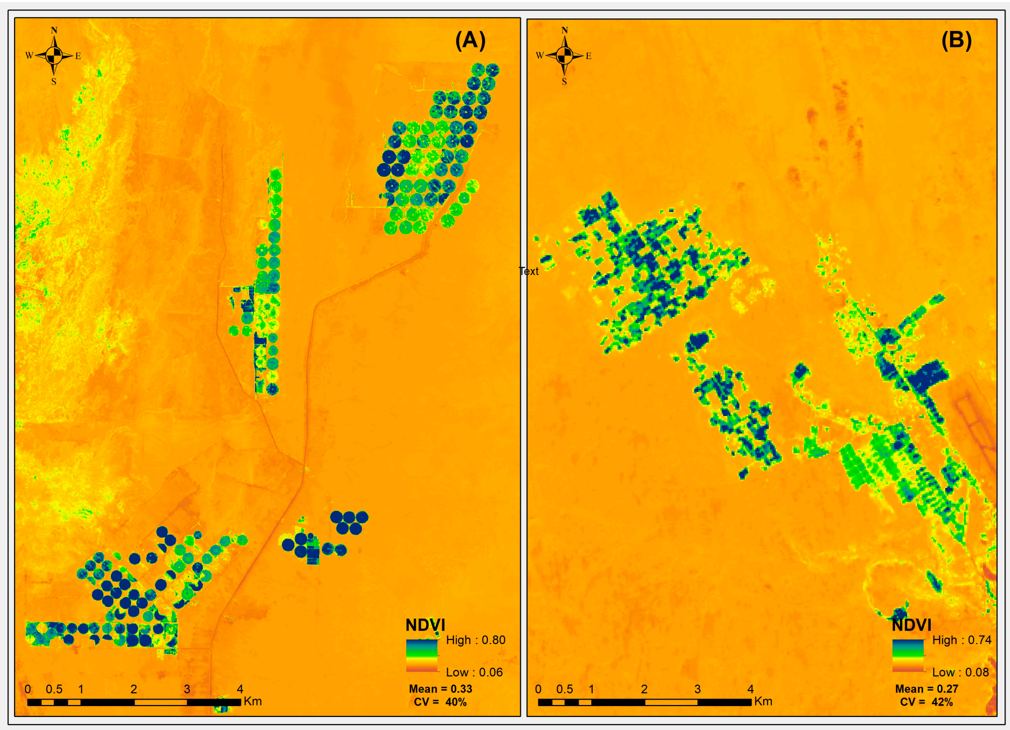

Figure 5. Mean NDVI at Toshka (**A**) and Abu Simbel (**B**) for the year 2014.

3.6. Study Limitations and Innovation

The study area has only one weather station used for calculating weather-based CWR and in SEBAL calibration. Thus, it is considered one of the limitations of this study. In addition, a crop map was not available for this study, which plays an important role in linking the proposed CWR using climate data and the actual CWR using remote sensing data. Therefore, we highly recommend this point in future studies. Despite that, the innovation of the study is integrating ALESarid-GIS, Ref-ET, and SEBAL models for selecting crop suitability and assessing its water requirements using weather and remote sensing data in a given area. Besides, we highly encourage to add some crops which are planted in the study area, but not included in ALESarid database (i.e., eggplant, courgettes, garlic, okra, spinach, corchorus, hibiscus, henna, sesame and fenugreek).

4. Conclusions

Crop type and water management must be compatible with land and water resources. When selecting cropping systems, several factors related to soil properties and water quality have to be considered, along with other climatic factors that may affect the physiological performance of each individual crop differently. ALESarid-GIS facilitates the selection of suitable crops to improve the estimation of irrigation crop water requirements based on crop suitability. Remote sensing techniques and the SEBAL model offer a great tool that can be used for estimating the ETa and support land and water management, especially in arid and semiarid regions of the world. Our results reveal that: (1) The highly suitable crops are alfalfa and sorghum (95%) followed by onion, wheat and barley (90%), sugar beet (80%), sugarcane, peppers and watermelons (70%), and pear (50%); (2) their weather-based CWR ranges from 804 to 1625 mm for wheat and berssem (5 cuts), respectively; and (3) satellite-based CWR spatial distribution for Toshka pivots irrigation system ranges between 10 and 1702 mm/year (mean = 821 mm/year), while this finding for Abu Simbel flood irrigation system it ranges from 16 to 1338 mm/year (mean = 557 mm/year). The findings of the present research may help decision-makers to plan and manage the future marginal land reclamation projects in Egypt and arid and semi-arid areas of the world. The concept of the current study can be applied to other sites of a similar subject.

Author Contributions: Conceptualization, H.S. and M.S., Data acquisition, A.E. Design of methodology H.S., M.A., and A.E. Writing and editing, M.S. and M.A. All authors have read and agreed to the published version of the manuscript.

Funding: This research was partially funded by Cairo University, Egypt.

Conflicts of Interest: The authors declare no conflict of interest.

Appendix A

Table A1. Coefficient parameters (a and b) of momentum roughness length (Z0m) and temperature differences (dT).

DOY	Z0m=exp[(a × NDVI/α)+b]		dT = (a × T_s) + b	
	a	b	a	b
51	5.02	−6.45	0.36	−107.5
83	4.99	−6.44	0.30	−88.91
131	5.13	−6.47	0.17	−50.55
147	5.11	−6.44	0.15	−45.36
163	5.05	−6.43	0.16	−48.33
179	4.88	−6.38	0.13	−40.58
195	5.06	−6.42	0.26	−79.56
211	5.07	−6.45	0.17	−51.52
227	4.88	−6.38	0.18	−55.86
243	5.02	−6.42	0.25	−76.85
259	4.99	−6.42	0.20	−62.17
275	4.94	−6.41	0.25	−73.90
291	4.78	−6.35	0.22	−66.47
307	4.98	−6.42	0.25	−76.29
339	5.25	−6.52	0.31	−92.15
355	4.96	−6.43	0.49	−142.51
Min.	4.78	−6.52	0.13	−142.51
Max.	5.25	−6.35	0.49	−40.58
Mean	5.01	−6.43	0.24	−72.41
SD	0.11	0.04	0.09	25.68
CV (%)	2.14	−0.57	37.21	−35.46

Note DOY, day of the year; Min, minimum; Max, maximum; SD, standard deviation; CV, coefficient of determination.

References

1. FAO. *Arid Zone Forestry: A Guide for Field Technicians*; Food and Agriculture Organization: Rome, Italy, 1989.
2. D'Odorico, P.; Bhattachan, A. Hydrologic variability in dryland regions: Impacts on ecosystem dynamics and food security. *Philos. Trans. R. Soc. B Biol. Sci.* **2012**, *367*, 3145–3157. [CrossRef] [PubMed]
3. Wheater, H.; Sorooshian, S.; Sharma, K.D. *Hydrological Modelling in Arid and Semi-Arid Areas*; Cambridge University Press: London, UK, 2007.
4. Camarasa-Belmonte, A.M.; Soriano, J. Empirical study of extreme rainfall intensity in a semi-arid environment at different time scales. *J. Arid Environ.* **2014**, *100–101*, 63–71. [CrossRef]
5. Williams, M. *Climate Change in Deserts: Past, Present and Future*; Cambridge University Press: London, UK, 2014.
6. Rossiter, D.G. ALES: A framework for land evaluation using a microcomputer. *Soil Use Manag.* **1990**, *6*, 7–20. [CrossRef]
7. De la Rosa, D.; Mayol, F.; Diaz-Pereira, E.; Fernandez, M.; de la Rosa, D., Jr. A land evaluation decision support system (MicroLEIS DSS) for agricultural soil protection: With special reference to the Mediterranean region. *Environ. Model. AMP Softw.* **2004**, *19*, 929–942. [CrossRef]
8. Akıncı, H.; Özalp, A.Y.; Turgut, B. Agricultural land use suitability analysis using GIS and AHP technique. *Comput. Electron. Agric.* **2013**, *97*, 71–82. [CrossRef]
9. Ali, R.R.; Shalaby, A. Sustainable agriculture in the arid desert west of the Nile Delta: A crop suitability and water requirements perspective. *Int. J. Soil Sci.* **2012**, *7*, 116–131. [CrossRef]
10. Abdel Kawy, W.A.; Abou El-Magd, I.H. Assessing crop water requirements on the bases of land suitability of the soils South El Farafra Oasis, Western Desert, Egypt. *Arab. J. Geosci.* **2013**, *6*, 2313–2328. [CrossRef]
11. Elnashar, A.F. Assessing Crop Suitability and Water Requirements of the Common Land Use in Egypt, Sudan and Ethiopia. Institute of African Research and Studies. Master's Thesis, Cairo University, Giza, Egypt, 2016.
12. Joshua, J.K.; Anyanwu, N.C.; Ahmed, A.J. Land suitability analysis for agricultural planning using GIS and multi criteria decision analysis approach in Greater Karu Urban Area, Nasarawa State, Nigeria. *Afr. J. Agric. Sci. Technol.* **2013**, *1*, 14–23.
13. Bozdag, A.; Yavuz, F.; Gunay, A.S. AHP and GIS based land suitability analysis for Cihanbeyli (Turkey) County. *Environ. Earth Sci.* **2016**, *75*, 813–827. [CrossRef]
14. Ghabour, T.K.; Ali, R.R.; Wahba, M.M.; El-Naka, E.A.; Selim, S.A. Spatial decision support system for land use management of newly reclaimed areas in arid regions. *Egypt. J. Remote Sens. Space Sci.* **2019**, *22*, 219–225. [CrossRef]
15. De la Rosa, D.; Moreno, J.A.; Garcia, L.V.; Almorza, J. MicroLEIS: A microcomputer-based Mediterranean land evaluation information system. *Soil Use Manag.* **1992**, *8*, 89–96. [CrossRef]
16. Yizengaw, S.; Verheye, W. Computer aided decision support system in land evaluation—A case study. *Agropedology* **1994**, *4*, 1–18.
17. Yizengaw, T.; Verheye, W. Application of computer captured knowledge in land evaluation, using ALES in central Ethiopia. *Geoderma* **1995**, *66*, 297–311. [CrossRef]
18. Ismail, H.A.; Bahnassy, M.H.; Abd El-Kawy, O.R. Integrating GIS and modelling for agricultural land suitability evaluation at East Wadi El-Natrun, Egypt. *Egypt. J. Soil Sci.* **2005**, *45*, 297–322.
19. Elsheikh, R.; Mohamed Shariff, A.R.B.; Amiri, F.; Ahmad, N.B.; Balasundram, S.K.; Soom, M.A.M. Agriculture Land Suitability Evaluator (ALSE): A decision and planning support tool for tropical and subtropical crops. *Comput. Electron. Agric.* **2013**, *93*, 98–110. [CrossRef]
20. Rossiter, D.G. A theoretical framework for land evaluation. *Geoderma* **1996**, *72*, 165–190. [CrossRef]
21. Rossiter, D.G. Biophysical models in land evaluation. In *Encyclopedia of Life Support Systems (EOLSS), Section 1.5 "Land Use and Land Cover"*; Verheye, W.H., Ed.; EOLSS Publishers Co. Ltd.: Oxford, UK, 2003; pp. 1–16.
22. El-Kawy, A.O.R.; Ismail, H.A.; Rod, J.K.; Suliman, A.S. A Developed GIS-based land evaluation model for agricultural land suitability assessments in arid and semi-arid regions. *Res. J. Agric. Biol. Sci.* **2010**, *6*, 589–599.
23. Wahab, M.A.; El Semary, M.A.; Ali, R.R.; Darwish, K.M. Land resources assessment for agricultural use in some areas west of Nile valley, Egypt. *J. Appl. Sci. Res.* **2013**, *9*, 4288–4298.
24. Darwish, K.M.; Abdel Kawy, W.A. Land suitability decision support for assessing land use changes in areas west of Nile Delta, Egypt. *Arab. J. Geosci.* **2014**, *7*, 865–875. [CrossRef]
25. Abd El-Kawy, O.R.; Flous, G.M.; Abdel-Kader, F.H.; Suliman, A.S. Land suitability analysis for crop cultivation in a newly developed area in Wadi Al-Natrun, Egypt. *Alex. Sci. Exch. J.* **2019**, *40*, 683–693. [CrossRef]
26. Mahmoud, H.; Binmiskeen, A.; Saad Moghanm, F. Land evaluation for crop production in the Banger El-Sokkar Region of Egypt using a geographic information system and ALES-arid Model. *Egypt. J. Soil Sci.* **2020**, *60*, 129–143. [CrossRef]
27. Bryla, D.R.; Trout, T.J.; Ayars, J.E. weighing lysimeters for developing crop coefficients and efficient irrigation practices for vegetable crops. *HortScience* **2010**, *45*, 1597–1604. [CrossRef]
28. Jia, X.; Dukes, M.D.; Jacobs, J.M. Bahiagrass crop coefficients from eddy correlation measurements in central Florida. *Irrig. Sci.* **2009**, *28*, 5–15. [CrossRef]
29. Pivec, J.; Brant, V.; Hamouzová, K. *Evapotranspiration and Transpiration Measurements in Crops and Weed Species by the Bowen Ratio and Sapflow Methods under the Rainless Region Conditions*; Gerosa, G., Ed.; InTech: London, UK, 2011. [CrossRef]
30. Allen, R.; Tasumi, M.; Trezza, R. Satellite-based energy balance for mapping evapotranspiration with internalized calibration (METRIC)-Model. *J. Irrig. Drain. Eng.* **2007**, *133*, 380–394. [CrossRef]

31. Morton, C.G.; Huntington, J.L.; Pohll, G.M.; Allen, R.G.; McGwire, K.C.; Bassett, S.D. Assessing calibration uncertainty and automation for estimating evapotranspiration from agricultural areas using METRIC. *J. Am. Water Resour. Assoc.* **2013**, *49*, 549–562. [CrossRef]
32. Tasumi, M.; Allen, R.G.; Trezza, R.; Wright, L. Satellite-based energy balance to assess within-population variance of crop coefficient curves. *J. Irrig. Drain. Eng.* **2005**, *131*, 94–109. [CrossRef]
33. El-Magd, I.A.; Tanton, T. Remote sensing and GIS for estimation of irrigation crop water demand. *Int. J. Remote Sens.* **2005**, *26*, 2359–2370. [CrossRef]
34. Allen, R.; Irmak, A.; Trezza, R.; Hendrickx, J.M.H.; Bastiaanssen, W.; Kjaersgaard, J. Satellite-based ET estimation in agriculture using SEBAL and METRIC. *Hydrol. Process.* **2011**, *25*, 4011–4027. [CrossRef]
35. Yang, Y.; Shang, S.; Jiang, L. Remote sensing temporal and spatial patterns of evapotranspiration and the responses to water management in a large irrigation district of North China. *Agric. For. Meteorol.* **2012**, *164*, 112–122. [CrossRef]
36. Fisher, J.B.; Melton, F.; Middleton, E.; Hain, C.; Anderson, M.; Allen, R.; McCabe, M.F.; Hook, S.; Baldocchi, D.; Townsend, P.A.; et al. The future of evapotranspiration: Global requirements for ecosystem functioning, carbon and climate feedbacks, agricultural management, and water resources. *Water Resour. Res.* **2017**, *53*, 2618–2626. [CrossRef]
37. Bastiaanssen, W.; Menenti, M.; Feddes, R.; Holtslag, A. A remote sensing surface energy balance algorithm for land (SEBAL): 1. Formulation. *J. Hydrol.* **1998**, *212–213*, 198–212. [CrossRef]
38. Su, Z. The Surface Energy Balance System (SEBS) for estimation of turbulent heat fluxes. *Hydrol. Earth Syst. Sci.* **2002**, *6*, 85–99. [CrossRef]
39. Senay, G.B. Satellite psychrometric formulation of the operational Simplified Surface Energy Balance (SSEBop) model for quantifying and mapping evapotranspiration. *Appl. Eng. Agric.* **2018**, *34*, 555–566. [CrossRef]
40. Anderson, M.C.; Norman, J.M.; Mecikalski, J.R.; Otkin, J.A.; Kustas, W.P. A climatological study of evapotranspiration and moisture stress across the continental United States based on thermal remote sensing: 1. Model formulation. *J. Geophys. Res. Atmos.* **2007**, *112*, D10117. [CrossRef]
41. Courault, D.; Seguin, B.; Olioso, A. Review on estimation of evapotranspiration from remote sensing data: From empirical to numerical modeling approaches. *Irrig. Drain. Syst.* **2005**, *19*, 223–249. [CrossRef]
42. Liou, Y.; Kar, S.K. Evapotranspiration estimation with remote sensing and various surface energy balance algorithms—A review. *Energies* **2014**, *7*, 2821–2849. [CrossRef]
43. Subedi, A.; Chávez, J.L. Crop evapotranspiration (ET) estimation models: A review and discussion of the applicability and limitations of ET methods. *J. Agric. Sci.* **2015**, *7*, 50–68. [CrossRef]
44. Zhang, K.; Kimball, J.S.; Running, S.W. A review of remote sensing based actual evapotranspiration estimation. *Wiley Interdiscip. Rev. Water* **2016**, *3*, 834–853. [CrossRef]
45. Bastiaanssen, W.; Pelgrum, H.; Wang, J.; Ma, Y.; Moreno, J.; Roerink, G.; van der Wal, T. A remote sensing surface energy balance algorithm for land (SEBAL): 2. Validation. *J. Hydrol.* **1998**, *212–213*, 213–229. [CrossRef]
46. Zamani Losgedaragh, S.; Rahimzadegan, M. Evaluation of SEBS, SEBAL, and METRIC models in estimation of the evaporation from the freshwater lakes (Case study: Amirkabir dam, Iran). *J. Hydrol.* **2018**, *561*, 523–531. [CrossRef]
47. Papadavid, G.; Perdikou, S.; Hadjimitsis, M.; Hadjimitsis, D. Remote sensing applications for planning irrigation management. The use of SEBAL methodology for estimating crop evapotranspiration in Cyprus. *Environ. Clim. Technol.* **2012**, *9*, 17–21. [CrossRef]
48. Bhattarai, N.; Dougherty, M.; Marzen, L.J.; Kalin, L. Validation of evaporation estimates from a modified surface energy balance algorithm for land (SEBAL) model in the south-eastern United States. *Remote Sens. Lett.* **2012**, *3*, 511–519. [CrossRef]
49. Jaafar, H.H.; Ahmad, F.A. Time series trends of Landsat-based ET using automated calibration in METRIC and SEBAL: The Bekaa Valley, Lebanon. *Remote Sens. Environ.* **2019**. [CrossRef]
50. Laipelt, L.; Ruhoff, A.L.; Fleischmann, A.S.; Kayser, R.H.B.; Kich, E.d.M.; da Rocha, H.R.; Neale, C.M.U. Assessment of an automated calibration of the SEBAL algorithm to estimate dry-season surface-energy partitioning in a forest–savanna transition in Brazil. *Remote Sens.* **2020**, *12*, 1108. [CrossRef]
51. USDA. *Soil Survey Field and Laboratory Methods Manual*; National Soil Survey Center, Natural Resources Conservation Service; U.S. Department of Agriculture: Lincoln, NE, USA, 2009.
52. Appel, M.; Lahn, F.; Buytaert, W.; Pebesma, E. Open and scalable analytics of large Earth observation datasets: From scenes to multidimensional arrays using SciDB and GDAL. *ISPRS J. Photogramm. Remote Sens.* **2018**, *138*, 47–56. [CrossRef]
53. ASCE-EWRI. *The ASCE Standardized Reference Evapotranspiration Equation*; ASCE-EWRI Standardization of Reference Evapotranspiration Task Committee Report; The American Society of Civil Engineers (ASCE): Washington, DC, USA, 2005; p. 216.
54. Allen, R. *REF-ET: Reference Evapotranspiration Calculation Software for FAO and ASCE Standardized Equations Version 4.1. for Windows*; University of Idaho: Moscow, ID, USA, 2015.
55. Allen, R.; Pereira, L.S.; Raes, D.; Smith, M. *Crop Evapotranspiration: Guidelines for Computing Crop Water Requirements*; Food and Agriculture Organization: Rome, Italy, 1998.
56. Waters, R.; Allen, R.; Tasumi, M.; Trezza, R.; Bastiaanssen, W. *SEBAL: Surface Energy Balance Algorithms for Land—Advanced Training and Users Manual Version 1.0*; The Idaho Department of Water Resources: Boise, ID, USA, 2002; p. 98.
57. Bastiaanssen, W.; Ahmad, M.-u.-D.; Chemin, Y. Satellite surveillance of evaporative depletion across the Indus basin. *Water Resour. Res.* **2002**, *38*, 1273. [CrossRef]

58. Bastiaanssen, W.; Noordman, E.; Pelgrum, H.; Davids, G.; Thoreson, B.; Allen, R. SEBAL model with remotely sensed data to improve water-resources management under actual field conditions. *J. Irrig. Drain. Eng.* **2005**, *131*, 85–93. [CrossRef]
59. Beg, A.A.F.; Al-Sulttani, A.H.; Ochtyra, A.; Jarocińska, A.; Marcinkowska, A. Estimation of evapotranspiration using SEBAL algorithm and Landsat-8 data-A case study: Tatra mountains region. *J. Geol. Resour. Eng.* **2016**, *6*, 257–270. [CrossRef]
60. Farah, H.; Bastiaanssen, W. Impact of spatial variations of land surface parameters on regional evaporation: A case study with remote sensing data. *Hydrol. Process.* **2001**, *15*, 1585–1607. [CrossRef]
61. Brutsaert, W.; Sugita, M. Application of self-preservation in the diurnal evolution of the surface energy budget to determine daily evaporation. *J. Geophys. Res.* **1992**, *97*, 18377–18382. [CrossRef]
62. Ahmad, M.D.; Biggs, T.; Turral, H.; Scott, C.A. Application of SEBAL approach and MODIS time-series to map vegetation water use patterns in the data scarce Krishna river basin of India. *Water Sci. Technol.* **2006**, *53*, 83–90. [CrossRef] [PubMed]
63. Bastiaanssen, W. SEBAL-based sensible and latent heat fluxes in the irrigated Gediz basin, Turkey. *J. Hydrol.* **2000**, *229*, 87–100. [CrossRef]
64. Khalifa, A.M. Mineralogical and Chemical Properties of Toshka Soils. Institute of African Research and Studies. Master's Thesis, Cairo University, Giza, Egypt, 2001.
65. Abbas, H.H.; El-Husseiny, O.H.; Mohamed, M.K.; Abuzaid, A.S. Land capability and suitability of some soils in Toshka area, Southwestern Egypt. *Ann. Agric. Sci. MoshtohorEgypt* **2010**, *48*, 1–12.
66. Hamzawy, M.M.H. Soil Studies in Lake Nasser Region Using Remote Sensing and GIS Capabilities. Ph.D. Thesis, Al-Azhar University, Cairo, Egypt, 2014.
67. Taghizadeh-Mehrjardi, R.; Nabiollahi, K.; Rasoli, L.; Kerry, R.; Scholten, T. Land suitability assessment and agricultural production sustainability using machine learning models. *Agronomy* **2020**, *10*, 573. [CrossRef]
68. FAO. *Water Quality for Agriculture*; Food and Agriculture Organization of the United Nations: Rome, Italy, 1985.
69. El-Mahdy, M.E.; Abbas, M.S.; Sobhy, H.M. Investigating the water quality of the water resources bank of egypt: Lake nasser. In *Conventional Water Resources and Agriculture in Egypt*; Negm, A.M., Ed.; Springer International Publishing: Cham, Swetzerland, 2019; pp. 639–655. [CrossRef]
70. Fayed, R.M.; Hussin, M.A.; Rizk, A.H.; Tawfik, T.A.; M Shreif, M.M. Effect of wells water quality on some soil properties and productivity in Toshka area. *J. Soil Sci. Agric. Eng.* **2010**, *1*, 873–881. [CrossRef]
71. IDMC. *Aswan Governorate Statistical Guide*; Information and Decision Making Center: Aswan, Aswan Governorate, Egypt, 2014. (In Arabic)
72. Hassan, F.O.; Salam, A.A.A.; Rashed, H.S.; Faid, A.M. Land evaluation and suitability of Hala'ib and Shalateen region, Egypt, by integrated use of GIS and remote sensing techniques. *Ann. Agric. Sci. Moshtohor.* **2017**, *55*, 151–162.
73. Brouwer, C.; Prins, K.; Heibloem, M. *Irrigation Water Management: Irrigation Scheduling*; Food and Agriculture Organization: Rome, Italy, 1989.
74. El-Marsafawy, S.M.; Eid, H.M. Estimation of water consumptive use for Egypt. In Proceedings of the Third Conference of On-Farm Irrigation and Agroclimatology, Cairo, Egypt, 25–27 January 1999.
75. Eid, H.M.; Ainer, N.G.; El-Marsafawy, S.M.; Khater, A.N. Crop water needs under different irrigation system in new land. In Proceedings of the Third Conference of On-Farm Irrigation and Agroclimatology, Cairo, Egypt, 25–27 January 1999.
76. Eid, H.M.; El-Marsafawy, S.M.; Abbas, F.A.; Ali, M.A.; Khater, I.N.; Eissa, M.M. Estimation of water needs for vegetable crops in the new land. *Meteorol. Res. Bull.* **2002**, *16*, 156–179.
77. Eid, H.M.; El-Marsafawy, S.M.; Ibrahim, M.M.; Eissa, M.M. Estimation of water needs for Orchard trees in the old land. *Meteorol. Res. Bull.* **2002**, *17*, 131–139.
78. Mahmoud, M.A.; El-Bably, A.Z. Crop water requirements and irrigation efficiencies in Egypt. In *Conventional Water Resources and Agriculture in Egypt*; Negm, A.M., Ed.; Springer International Publishing: Cham, Swetzerland, 2019; pp. 471–487. [CrossRef]
79. Calera, A.; Campos, I.; Osann, A.; D'Urso, G.; Menenti, M. Remote sensing for crop water management: From ET modelling to services for the end users. *Sensors* **2017**, *17*, 1104. [CrossRef]
80. Abd El-Hady, A.M.; Abdelaty, E.F. GIS—Comprehensive analytical approach for soil use by linking crop soil suitability to soil management and reclamation. *Alex. Sci. Exch. J.* **2019**, *40*, 60–81. [CrossRef]
81. Paula, A.C.P.d.; Silva, C.L.d.; Rodrigues, L.N.; Scherer-Warren, M. Performance of the SSEBop model in the estimation of the actual evapotranspiration of soybean and bean crops. *Pesqui. Agropecuária Bras.* **2019**, *54*. [CrossRef]
82. Biro, K.; Zeineldin, F.; Al-Hajhoj, M.R.; Dinar, H.A. Estimating irrigation water use for date palm using remote sensing over an Oasis in arid region. *Iraqi J. Agric. Sci.* **2020**, *51*, 1173–1187. [CrossRef]
83. Sun, Z.; Wei, B.; Su, W.; Shen, W.; Wang, C.; You, D.; Liu, Z. Evapotranspiration estimation based on the SEBAL model in the Nansi Lake Wetland of China. *Math. Comput. Model.* **2011**, *54*, 1086–1092. [CrossRef]